Colloids and Surfaces A 577 (2019) 158–166

Contents lists available at ScienceDirect

Colloids and Surfaces A

journal homepage: www.elsevier.com/locate/colsurfa

Spontaneous clay Pickering emulsification

Wen Song[a,b,*], Anthony R. Kovscek[a]

[a] Department of Energy Resources Engineering, Stanford University, Stanford, USA
[b] Department of Petroleum and Geosystems Engineering, University of Texas at Austin, Austin, USA

GRAPHICAL ABSTRACT

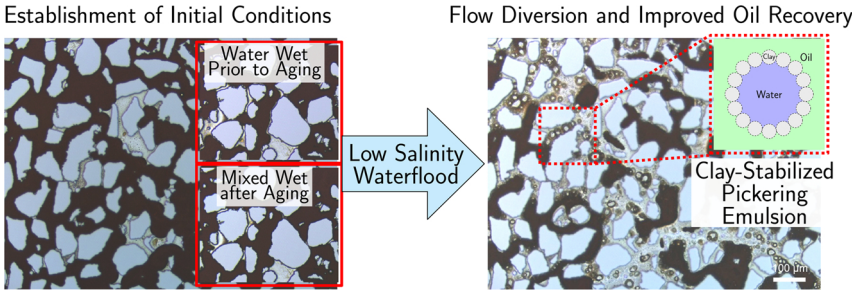

ARTICLE INFO

Keywords:
Low salinity waterflooding
Pickering emulsion
Clay nanoparticles

ABSTRACT

Clay-rich sandstone formations contain vast deposits of petroleum resources. Low salinity waterflooding presents a low-energy, low-environmental impact method to improve oil recovery from these systems. Fundamental mechanisms dictating improved oil recovery at low salinity conditions are not well-understood currently. This study investigates low salinity waterflooding at the pore-level to delineate fundamental mechanisms underlying oil recovery. Clay-functionalized, two-dimensional micromodels are used to provide direct visual observations of crude oil, brine, and clay particle interactions within the pore-space. Using this microvisual approach, establishment of initial reservoir conditions shows wettability evolution of the initially water-wet system towards a mixed-wet condition due to clay-particle interactions with the reservoir fluids, i.e., crude oil and brine. Pore-scale behavior during low salinity waterflooding shows spontaneous emulsification of the crude oil and brine. Specifically, the emulsions generated are Pickering type stabilized by the clay particles that were mobilized at salinities below the critical salt concentration (CSC). Spontaneous generation of the stable Pickering emulsions reduces mobility through preferential flow paths, thereby resulting in flow diversion of subsequent injection fluids to mobilize oil-filled pores. Leveraging the stability of the Pickering emulsions, a sequential salinity cycling method is developed to improve overall oil recovery by an additional 8% of the original oil in place. Flow diversion due to spontaneous Pickering emulsification in preferential flow paths observed here provides fundamental insight to the design and application of low energy-input, low environmental-impacts techniques in the field.

1. Introduction

Clay-rich sandstones contain vast deposits of global petroleum resources. Recovery of oil from these systems, however, is often limited [1]. Low salinity waterflooding, the injection of brine that is reduced in salinity compared to the original reservoir formation brine, presents an opportunity to improve overall oil recovery significantly [2,1,3–8]. Specifically, low salinity brine injection is of industrial interest due to

* Corresponding author.

https://doi.org/10.1016/j.colsurfa.2019.05.030
Received 20 January 2019; Received in revised form 9 May 2019; Accepted 11 May 2019
Available online 14 May 2019
0927-7757/

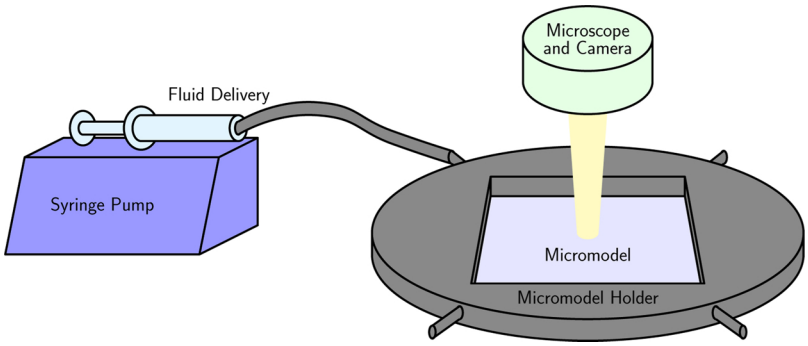

Fig. 1. Fluid delivery and visualization setup used in experiments. Brine and crude oil were delivered to the micromodel using the syringe pump. Pore-scale fluid behavior was monitored in real-time and fluid distributions across the micromodel were characterized using the microscope and camera setup. The fluids were delivered at ambient conditions.

its relatively low economic requirements as well as its ability to recover oil without significant energy or environmental impacts. Results from laboratory- and field-scale experiments, however, lack agreement.

Fundamental understanding of the underlying mechanics that dictate the improvements in oil recovery with low salinity brine injection, i.e., the low salinity effect, must be understood to optimize large-scale field-level implementation. Several mechanisms have thus far been suggested in an attempt to explain the low salinity effect. Specifically, three of the proposed mechanisms include (i) fines migration, whereby clay particles are mobilized in the pore-space and alter the overall wettability of the rock [2]; (ii) multicomponent ion exchange (MIE), in which the adsorbed charged components of the crude oil are replaced by an aqueous-phase ion such that the adsorbed oil molecules are released into the free-flowing phase [9]; and (iii) saponification, or, the generation of emulsions, due to the release of naturally present surface-active agents (surfactants) from the crude oil at the oil-brine interface [10]. Lack of agreement in the literature on the role of each proposed mechanism in inducing the low salinity effect necessitates mechanistic studies at the fundamental scale.

Fundamental behavior of petroleum reservoirs is dictated by pore-scale dynamics due to their porous nature [11]. Direct pore-level understanding of fluid transport through petroleum reservoirs has been limited due to the opacity and heterogeneity of rock. Advances to in-situ visualization techniques such as X-ray computed tomography (CT) has enabled observations of fluid distributions in real rock samples [12–15]. Spatiotemporal resolution of such techniques, however, is poor in comparison to those required to delineate the fundamental pore-scale dynamics.

Microfluidic systems have emerged as a fundamental tool for the direct visual study of petroleum systems behavior at the fundamental pore-scale. Specifically, micromodels, microfluidic platforms that have representative pore geometry of real rock, lend direct insight into pore-scale mechanisms by allowing real-time, micro-scale visualization [16,11]. Current state-of-the-art techniques for micromodel fabrication imprint rock pore geometry into silicon wafers through plasma etching, and the etched silicon wafer is subsequently bonded anodically with glass to enable flow and direct visualization [16]. Micromodel surfaces are oxidized to form SiO_2. Most recently, real-rock microfluidics [17] were developed to replicate the rock material more closely. Specifically, pore geometries have been etched into real-rock substrates such as calcite [17], shale [18], and coal [19]. Further, glass- and silicon-based microfluidics have been surface-functionalized with minerals such as clay [20,21] and calcite [22,23] to enable direct visual observation of fluid transport through and interactions with real rock material.

In this work, clay-functionalized micromodels are used to investigate the interactions between crude oil, brine, and clay particles that underlie the low salinity effect in clay-rich sandstones. The clay-functionalized micromodel is initialized to representative conditions by formation brine and crude oil injection, respectively, and by aging to allow for sufficient equilibration. The crude oil used is of industrial interest. Wettability changes to the pore space as a result of the clay particles are monitored. Pore-scale dynamics due to the injection of brines at high and low salinities were visualized directly through a microscope. Surprisingly, spontaneous generation of emulsions 5–30 μm in diameter were observed at very low salinity (i.e., freshwater) conditions throughout the preferential flow paths. We determine stable emulsions to be a result of the mobilized clay particles that stabilize the water-oil interface, thereby forming stable Pickering emulsions. The presence of the stable emulsions is leveraged to design a salinity cycling scheme that further improves overall oil recovery by an additional 8.5% original oil in place (OOIP).

2. Experimental methods

Experimental investigation of crude oil, brine, and clay interactions were conducted at the microscopic pore-scale and at the bulk scale. The following sections describe the pore- and bulk-scale methods taken, respectively.

2.1. Direct visualization of pore-scale dynamics

Direct, real-time visualization of pore-scale dynamics was enabled by a geochemically-representative micromodel, fluid delivery system, and a confocal microscope and camera (Sensofar S neox, Fig. 1). Clay-functionalized micromodels with representative pore geometry and surface properties of real reservoir rock were used to visualize pore-scale oil recovery dynamics in clay-rich sandstones. The clay-functionalization method follows the process described by Song and Kovscek [20,21]. Kaolinite clay (Kaolin, K2-500, Fisher Scientific) was used in this work due to its mobility with decreasing salinity and to mimic the target reservoir properties. Pore geometry patterns were etched into a silicon wafer using standard photolithography and plasma etching techniques (see Buchgraber [24] for details). Specifically, the micromodels follow a sandstone grain pattern obtained from binarized thin-section images of real sandstone. Inlet and outlet ports were drilled using a diamond drill bit to enable fluid delivery. Optically flat borosilicate glass was bonded anodically to the etched wafer to enable flow confinement and direct visualization [16].

Fluids used in this study correspond to a specific clay-rich sandstone reservoir of industrial relevance. The composition of the formation brine is listed in Table 1. Properties of the crude oil are shown in Table 2.

To replicate natural geological deposition, the clay-functionalized micromodel was first saturated with the formation brine (Fig. 2a).

Table 1
Composition of brine used to simulate initial reservoir conditions.

Analytical grade reagents	Concentration (g/L)
$CaCl_2{\cdot}2H_2O$ (Calcium chloride dihydrate)	0.183
$MgCl_2{\cdot}6H_2O$ (Magnesium chloride hexahydrate)	0.585
NaCl (Sodium chloride)	20.461
KCl (Potassium chloride)	0.611
Na_2SO_4 (Sodium sulfate)	0.109

Table 2
Crude oil characterization [25].

Crude oil properties	Value
Acid number (mg/g)	2.36
Base number (mg/g)	6.02
Asphaltene content (wt%)	2.69
Density (°API)	21
Viscosity at 22.8 °C (cP)	105.7

Crude oil was injected at ~1 m/day until residual water saturation was reached to mimic the process of oil migration into the reservoir (Fig. 2b).

The oil- and brine-filled micromodel was then submerged under crude oil at ambient conditions for two weeks to allow for sufficient interactions and equilibration between the phases (Fig. 2c). This is referred to as aging. The aged micromodel is taken as the initial condition, analogous to the industrial oil reservoir that this study is modeled around.

In keeping with industrial practices, several pore-volumes of high salinity brine (10 000 ppm NaCl) were injected into the aged micromodel to standardize the model system with secondary recovery processes commonly practiced in the industry (Fig. 2d). Low salinity brine (4000 ppm NaCl) was injected to study the dynamics of the clay-rich sandstone system during low salinity waterflooding (Fig. 2e). Brine with 4000 ppm NaCl was chosen here in accordance with the critical salt concentration for kaolinite mobilization found by Song and Kovscek [20] to investigate the importance of clay during low salinity waterflooding.

Freshwater (i.e., deionized water) was injected to investigate the effect of reduced salinity on overall oil recovery from the clay-rich sandstone model rock (Fig. 2f). All fluids were injected into the micromodel at a nominal velocity of 1 m/day to represent realistic subsurface flow conditions. Fluids were delivered using a syringe (BD 60 mL syringe, 309653) and syringe pump (Harvard Apparatus, Holliston, MA) at ambient conditions. Microvisual imaging was achieved immediately following each injection process using a confocal microscope (Sensofar Sneox 3D optical profiler). Images were captured at 25 fixed locations across the micromodel to minimize pore-scale variations. Fluid phases from the captured pore-scale images were segmented to quantify the fluid saturations and oil recoveries from the clay-rich sandstone model system.

2.2. Bulk-scale measurements

Interactions between crude oil, brine, and clay were characterized at the bulk scale. Specifically, emulsification with and without clay was tested using the crude oil (Table 1), the formation brine (Table 2), and deionized (DI) water through a simple shake-test in glass scintillation

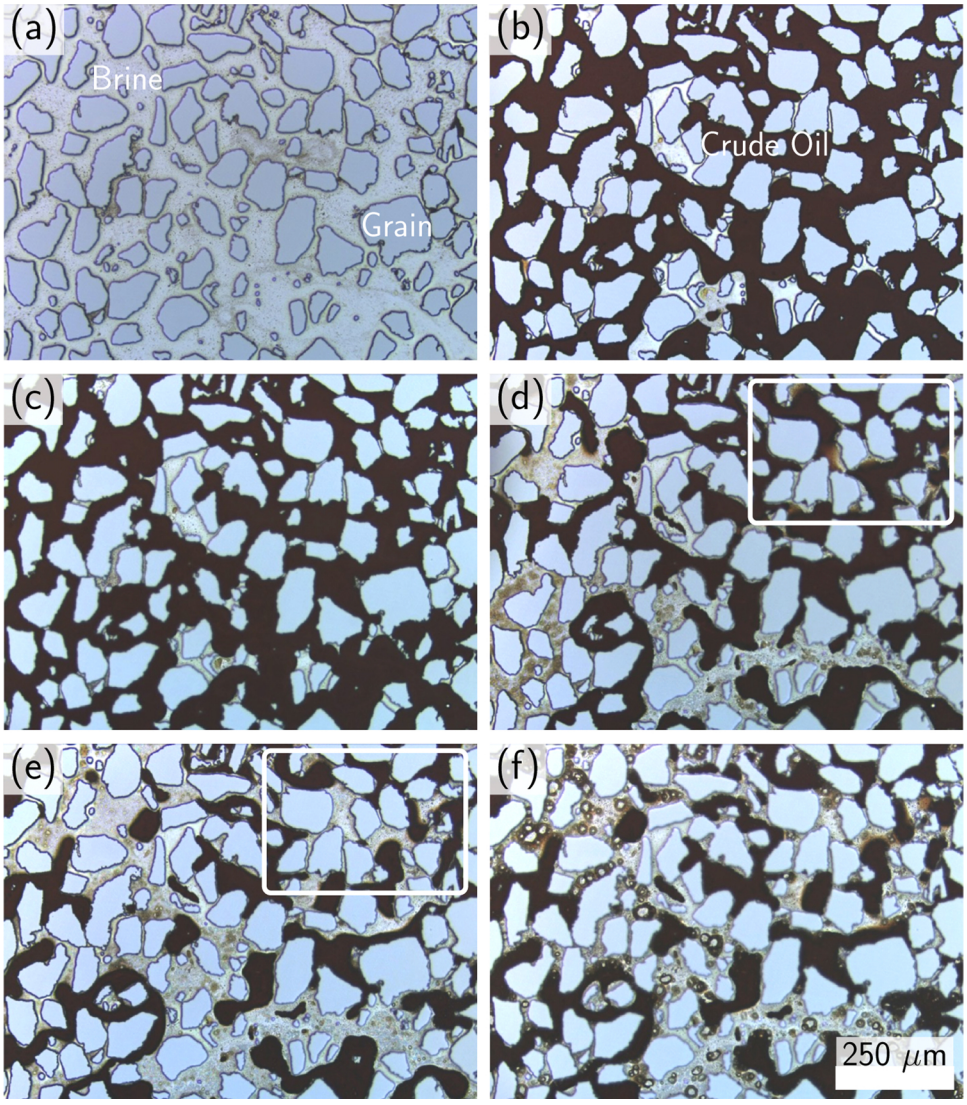

Fig. 2. Pore-level dynamics of the micromodel. (a) Clay-functionalized micromodel is saturated with formation brine (see Table 1 for composition) to mimic in-situ conditions. (b) Crude oil (see Table 2 for properties) corresponding to the formation brine is injected until the residual water saturation is reached to mimic the process of petroleum migration into the reservoir. (c) The micromodel is aged for two weeks to allow for the crude oil, brine, and solids to interact and equilibrate. This is the initial reservoir condition. (d) Initial high salinity brine (10 000 ppm NaCl) is injected to benchmark the experiment with secondary recovery results. (e) Improved oil recovery (~6.5% OOIP) is observed following low salinity brine (4000 ppm NaCl) injection. (f) Large (diameter ~5–30 μm) emulsions form throughout the pore-space during injection of deionized (DI) water. Emulsions are formed spontaneously throughout the preferential flow paths along the water–oil interfaces.

vials (20 mL Borosilicate Scintillation Vials, DWK Life Sciences Wheaton). Clay contents were varied for fixed water–oil ratios to investigate the minimum clay presence required to generate stable emulsions. Specifically, clay contents were varied from zero to 4.78 wt % in DI water with crude oil mixtures, and zero to 4.68 wt% in reservoir brine with crude oil mixtures. The vials of brine/DI water, crude oil, and/or clay were shaken vigorously for 1 minute and allowed to equilibrate. The emulsification process, or lackthereof, was monitored over time and emulsions sizes, if available, were characterized.

3. Results and discussion

Aging is discussed first followed by oil recovery.

3.1. Aging

Clay-functionalized micromodels with representative geometric and surface characteristics of real clay-rich sandstone (see Song and Kovscek [20] for validation study) were saturated with reservoir formation brine (geological deposition, Fig. 2a) and crude oil (crude oil migration, Fig. 2b) to visualize the effects of aging. Immediately following crude-oil migration, the clay-functionalized micromodel was strongly water-wet, as in silicon-based systems. Recall that petroleum fluids migrate to, accumulate, and reside in subsurface reservoirs over geological time (i.e., on the order of ~10s to 100s of million years). To achieve more realistic initial reservoir conditions, the model system was aged for two weeks to replicate the equilibration process underground to achieve representative initial reservoir conditions. Two weeks were deemed sufficient through monitoring of fluid distribution over time, in agreement with established practice [26,27].

Importantly, a mixed-wet condition is observed in the aged micromodel, away from the initial strongly water-wet condition. Equilibration between the fluid and solid constituents, i.e., aging, showed fluid redistribution from an initially water-wet condition (Fig. 3a) towards one that is more mixed-wet (Fig. 3b,c). Specifically, immediately following crude oil introduction to the system, water is found in the smallest pores and macroscopic water films line the grains (Fig. 3a). This is a classic example of the strongly water-wet condition. After aging, however, invasion of moderate-sized pores by crude oil (dashed box in Fig. 3a,b) and disappearance of the macroscopic water films are observed (Fig. 3b). The altered state at the end of aging is attributed to crude-oil, brine, and clay interactions. Specifically, charged edges of kaolinite clay particles attract charged components in the crude oil and hence alter the pore region towards oil-wetness. Mixed-wettability in the aged micromodel is further validated through observation of irregular water-oil interfaces due to pinning (Fig. 3c,i) and thin oil-films (Fig. 3c,ii). These results are consistent with the scenario for development of mixed-wettability [28] and are comparable to mixed-wettability of real clay-rich sandstone at initial reservoir conditions [1].

3.2. Oil recovery

Upon aging, the micromodel system is deemed representative of initial reservoir conditions. Injection of high salinity (10 000 ppm NaCl) brine displaced some of the crude oil and created preferential flow paths through the porous medium (Fig. 2d). Connected groups of water-saturated pores enable flow preference for the injection brine, and thus the bypass of oil-filled pores. Oil from the bypassed pores is not recovered. Notice, however, that not all oil-filled pores are bypassed pores, but instead are pores where the oil-wet pore-surfaces have retained the crude oil. This is especially apparent when comparing the boxed region in Fig. 2d after the high salinity waterflood to the corresponding region at initial reservoir conditions in Fig. 2c.

As a means to improve oil recovery from clay-rich sandstone reservoirs, low salinity waterflooding presents a method that minimizes the environmental and energetic impact associated with oil recovery. Of industrial interest, low salinity (4000 ppm NaCl) brine injection resulted in an increase in oil recovery, i.e., less oil saturation, from the micromodel system (Fig. 2e). With the low salinity brine, the wettability of the pore surfaces appear to shift from a mixed-wet condition to a water-wet condition. Specifically, development of macroscopic water films and removal of the thick residual oil films following low salinity brine injection (Fig. 2e, boxed region) serve as direct evidence. It is worth noting that the concentration of the low salinity brine chosen here corresponds to the critical salt concentration (CSC) that was measured for kaolinite clay particle mobilization in this micromodel system (see Song and Kovscek for details [20]) and that clay particles are mobilized in this system (see Song and Kovscek for details [21]).

Sensitivity of oil recovery to injection brine salinity was delineated with a tertiary injection of freshwater (DI water, Fig. 2f). Surprisingly, water-in-oil emulsions formed spontaneously throughout the micromodel. The emulsions were large (diameter ~5–30 μm) and populated the preferential flow paths forged during the high and initial low salinity brine injections. Unlike the small (diameter < 1 μm) emulsions due to the release of surface-active components at the oil-water interface (Fig. 5a) postulated previously [10], the emulsions generated in the present system are much larger in size.

Equilibration of the spontaneously generated emulsions shows that the emulsions are stable (Fig. 4). Emulsion surfaces appear rigid in structure, unlike surfactant-stabilized emulsions. Recall that the critical salt concentration (CSC) for kaolinite clay particle detachment and mobilization in this micromodel system is 4000 ppm NaCl. In other words, salinities below the CSC, as in the current system, results in an abundance of mobile detached clay particles.

The stability of the emulsions combined with its spontanous generation, its rigidity, and the availability of mobile clay particles in the low salinity pore space leads to the conclusion that the emulsions generated are of Pickering type (Fig. 5b). Pickering emulsions are those stabilized by the charged surfaces of particles at the fluid interface [29,30]. In the present system, mobile kaolinite clay particles, on the order of μm, serve as the stabilizing agents. Recall that kaolinite clay particles have charged edges by nature [31].

Comparison between clay-present and clay-absent systems at both the microscopic pore-scale and at the bulk-scale confirm the spontaneous generation of Pickering emulsions (Fig. 6). Specifically, in the absence of clay, a clean, distinct interface between the crude oil phase and the aqueous phase is observed at both the pore-level (Fig. 6a) and at the bulk-level (Fig. 6c). No emulsions were generated without clay particles present, as expected for this surfactant-poor crude oil-brine system. In the presence of clay, however, Pickering emulsions were generated at both the pore-scale (Fig. 6b) and the bulk-scale (Fig. 6d). Bulk- and pore-scale Pickering emulsions, importantly, have been stable since January 2016.

Due to the requirement of clay-particle availability on the formation of Pickering emulsions, emulsification as a function of clay content was investigated in bulk (Fig. 7) as a proxy for the pore-scale dynamics. Specifically, fixed volumes of aqueous phase (reservoir brine or DI water) and crude oil were added to varying kaolinite clay masses to delineate the impact of clay content and salinity on Pickering emulsification. For both brine/crude-oil and freshwater/crude-oil systems, a minimum clay content was required to generate a stable emulsion. In the case of crude oil with DI water, the minimum clay content required for stable Pickering emulsification was 1.64 wt% kaolinite (Fig. 7a,c). Crude oil and reservoir brine systems, however, required less clay (0.81 wt% kaolinite) to generate stable Pickering emulsions (Fig. 7b,c). The reduced requirement on clay content may be explained by the increased ion availability due to the dissolved salts. Interestingly, the sizes of the Pickering emulsions generated in both brine/crude-oil and freshwater/crude-oil systems decrease with increasing clay availability (Fig. 7c).

Decreased emulsion sizes with increasing clay availability may explain some core-scale observations of increased oil recovery with clay

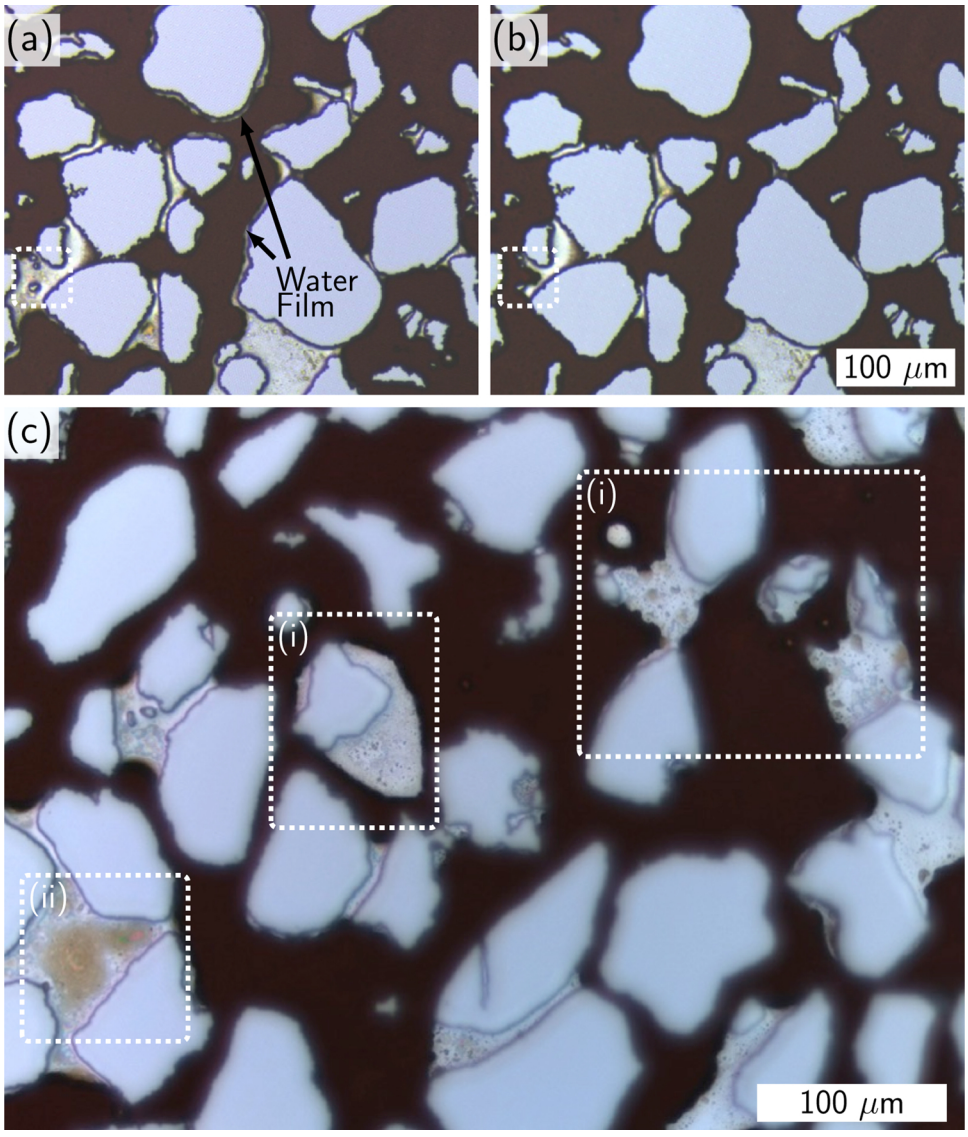

Fig. 3. Transition to mixed-wet behavior at the pore-scale due to aging. (a) Prior to aging, water resides in smallest pores and macroscopic water films surround grains, consistent with water-wet systems. (b) Following aging, macroscopic water films are no longer visible due to crude-oil interactions with clay. Mixed-wet behavior is further exemplified by crude oil displacement of brine in smaller pore-spaces (dashed box areas in (a) and (b)). (c) Mixed-wettability at the pore-scale is evident through observation of irregularly-shaped water-oil interfaces due to interfacial pinning on the clay particles (c,i), presence of thin oil films on the pore surface (c,ii), and occupancy of oil in smaller pore spaces (a,b, dashed boxes).

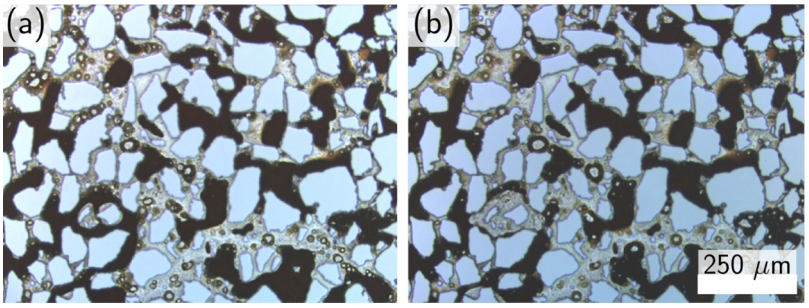

Fig. 4. Stability of 5–30 μm diameter emulsions at the pore-scale. (a) Emulsions throughout the preferential flow paths after freshwater injection. (b) Emulsions are stable after one week of equilibration.

content from the literature. Specifically, generation and residence of emulsions in the preferential flow paths create pressure buildups across those paths as a result of the large number of interfaces, and thus, capillary forces needed to be overcome for flow. Presence of high clay content in the reservoir enables the formation of Pickering emulsions of smaller diameters in the preferential flow paths. Dense populations of small emulsions in the preferential flow paths exacerbate the flow blockage through the water-saturated preferential flow paths by increasing the number of interfaces present.

The resulting resistance to pore-scale flow due to increased numbers of interfaces from small, dense emulsions thus reduces the local relative permeability of subsequent injection fluids. As a result, subsequent

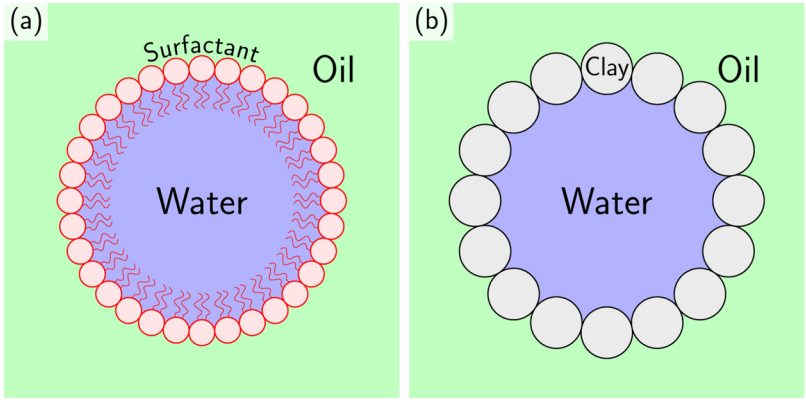

Fig. 5. Cartoon illustrations of the emulsion stabilizing agents. (a) Surface-active components (surfactant) stabilized emulsions due to added crude oil and brine chemistry. This is the type that has been reported previously to aid in low salinity improved oil recovery [10]. (b) Pickering emulsions, as observed, are stabilized due to charged surfaces of the clay particles that have been mobilized at salinities below the CSC for clay particle detachment (i.e., at low salinities).

injection fluid, such as brine, is diverted to pockets of the continuous crude oil phase with few interfaces to overcome. The macroscopic pressure gradient is largely unchanged because of the flow diversion mechanism. That is, the emulsification of the previous preferential flow paths forces fluids to forge new paths through the oil-filled pores. The pressure required to overcome a single interface, in comparison to that required in the emulsion-filled pores, is akin to the macroscopic pressure gradient at initial high salinity conditions. This may explain some field observations that show the lack of clay production and pressure buildup with increased oil recovery under low salinity conditions [9,32].

The combined spontaneous Pickering emulsification and flow diversion mechanisms here enable a tertiary increase in oil production from the system. Pore-scale micromodel experiments show that with subsequent injection of high salinity (20 000 ppm) brine, overall oil saturation in the system is reduced. In other words, overall oil recovery is increased.

Direct visual quantification of oil recovery from the clay-rich sandstone system is achieved through imaging and image processing. Representative averages were obtained by imaging at 25 fixed locations across the micromodel (Fig. 8a). Images were taken at each specified location following each injection process to track the evolution of the local fluid distribution at initial reservoir conditions (Fig. 8b,i), following the high salinity brine injection (Fig. 8b,ii), the low salinity 4000 ppm brine injection (Fig. 8b,iii), and the freshwater Pickering emulsification and subsequent high salinity brine injection (Fig. 8b,iv).

Image sets from each location were segmented (Fig. 8c) to delineate the oil (green), brine (blue), and solid (black) phases. The segmented images enable direct calculation of fluid phase saturations, i.e., oil recovery factors, of each location after each injection process. The two-dimensional nature of the micromodel enables quantification of volumetric saturations of crude oil, $S_o = V_o/V_{\text{pore}} = A_o/(A_o + A_w)$, and brine, $S_w = 1 - S_o$, directly from the images. Here, the volumes of oil, V_o, and pore space, $V_{\text{pore}} = V_o + V_w$, are determined from the areas that the brine and oil occupy. Oil recoveries following each injection process are averaged across the micromodel to determine the overall oil recovery

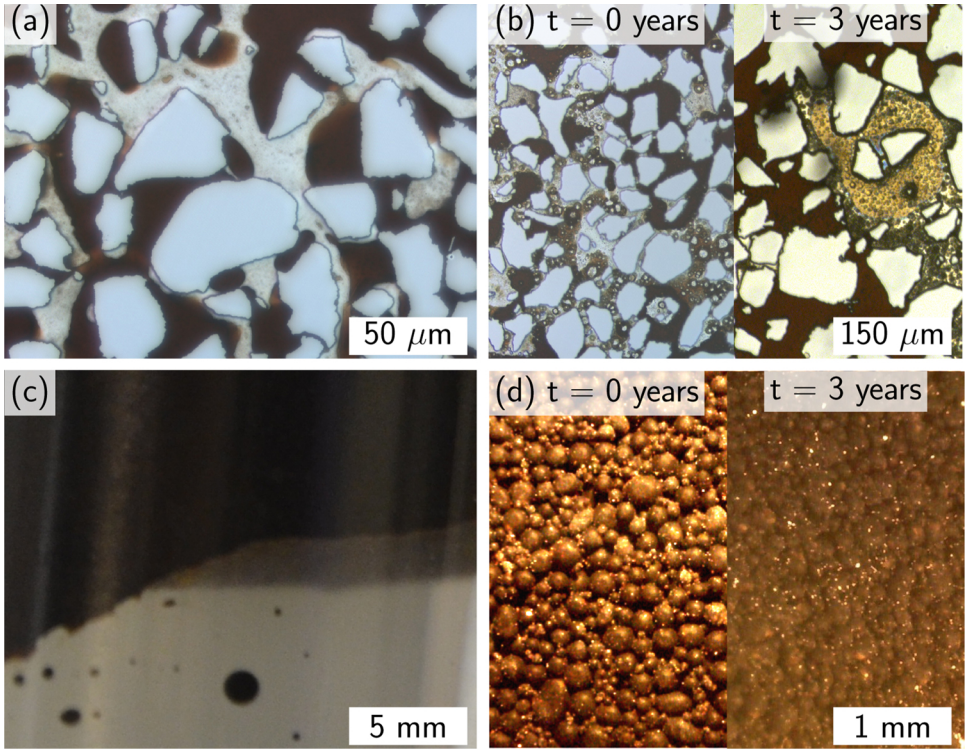

Fig. 6. Comparison of crude oil - brine system in the absence and presence of clay. Pore-scale micromodel experiments show clean water-oil interfaces in the absence of clay (a) and stable emulsions in the presence of clay (b), respectively. Bulk experiments show that in the absence of clay (c), brine and the crude oil prefer to reside in their individual phases, i.e., no emulsions are formed. In the presence of clay (d), however, stable Pickering emulsions are formed. The Pickering emulsions are stable over three years (b,d). We do not add surfactant or any other stabilizing agent to the oil-water system, and thus no stable emulsions were formed in the absence of clay (a, c). Charged clay-particle surfaces act to stabilize the Pickering emulsions observed at both bulk- and pore-scales (b, d).

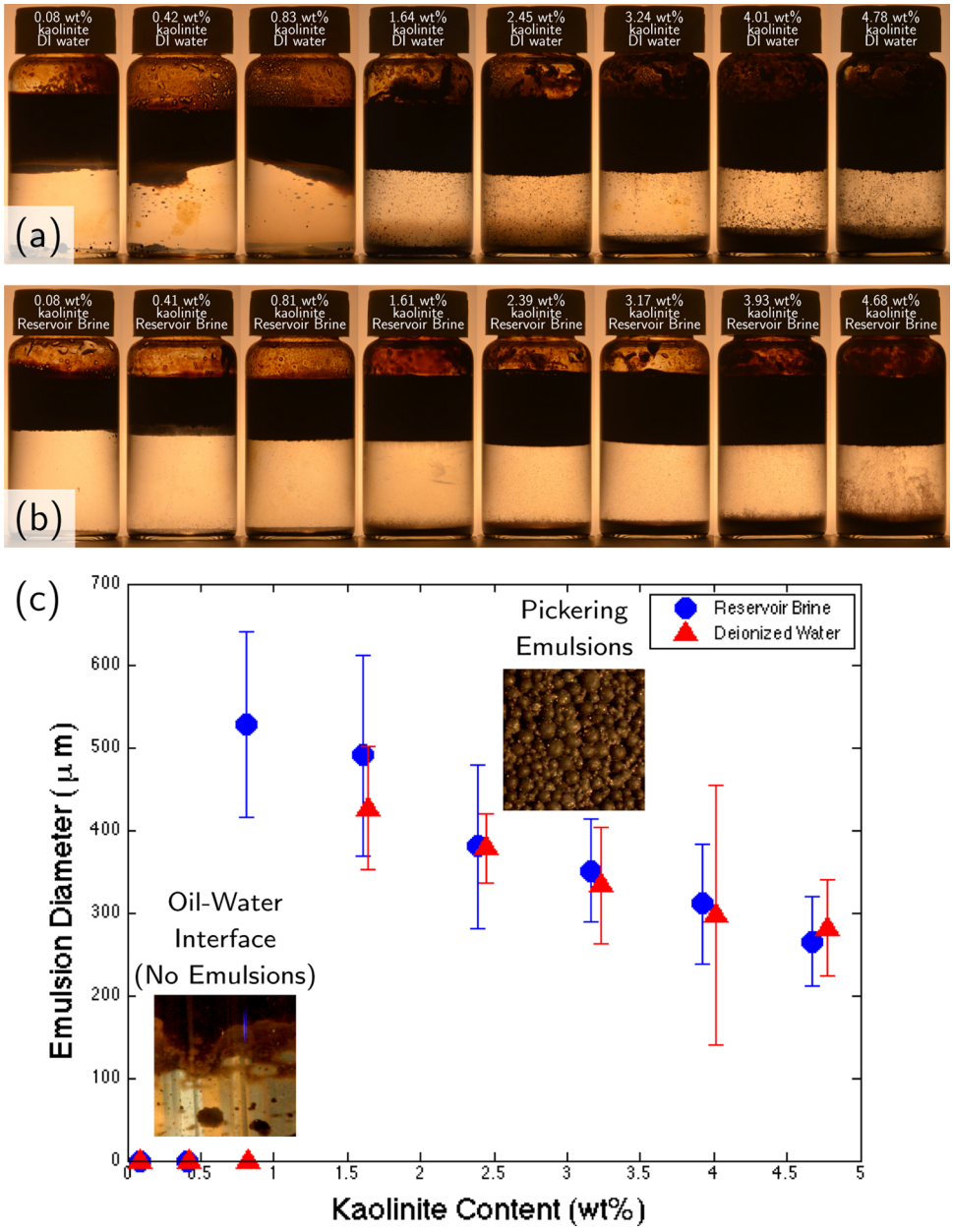

Fig. 7. Pickering emulsification as a function of clay content in bulk-scale shake tests. (a) Emulsification between crude oil and freshwater. No emulsions were formed for clay contents below 1.64 wt%. (b) Emulsification between crude oil and the reservoir brine. No emulsions were formed for clay contents below 0.81 wt%. (c) Characterization of emulsions sizes as a function of kaolinite clay content shows a minimum clay content to form stable emulsions in the system, and that emulsions sizes decrease with increasing clay availability.

(Fig. 8d). In this work, we find that the initial high salinity 10 000 ppm waterflood recovered ~ 38% of the original oil in place (OOIP), consistent with core- and field-scale studies [33]. Traditional low salinity 4000 ppm brine injection increased overall oil recovery by ~6.5% OOIP, again corroborated by core-flooding experiments [33]. The new salinity cycling method that we implement here, whereby freshwater is injected to mobilize clay particles and to generate stable Pickering emulsions spontaneously that block preferential flow paths and divert flow towards oil-filled pores followed by an additional high salinity flood, increased the overall oil recovery by an additional ~8% OOIP.

4. Conclusion

We delineate pore-scale dynamics underlying the presence of clay in crude-oil and brine systems. Specifically, we observe directly the alteration of pore-surface wettability due to the presence of clay. We observe the evolution of mixed-wet surfaces where oil films exist and are retained, and the absence of macroscopic water films as in strongly water-wet systems. Fundamental mechanisms underlying the low salinity effect in clay-rich sandstone were investigated using the mixed-wet clay-functionalized micromodel. In particular, wettability appears to shift towards water-wetness under low salinity (4000 ppm) conditions, evidenced by the disappearance of thick oil films and the appearance of

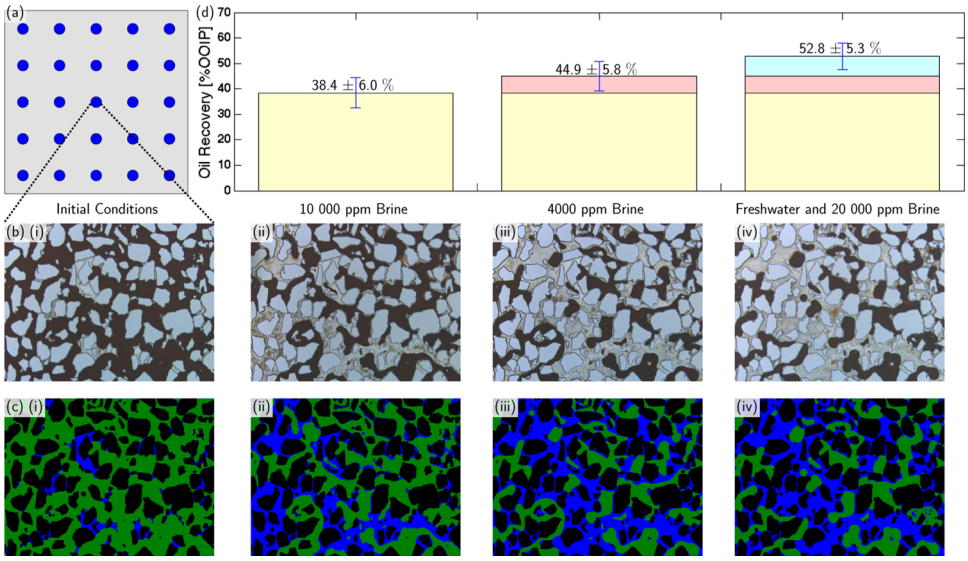

Fig. 8. Quantification of oil recovery from the clay-rich sandstone model system. (a) Images are taken at 25 fixed locations across the micromodel after each injection process to obtain a pore-averaged oil recovery factor. (b) Pore-level images of crude oil and brine distribution in the micromodel at initial conditions (i), following the initial 10 000 ppm high salinity brine injection (ii), following the 4000 ppm low salinity brine injection (iii), and following the freshwater and subsequent high salinity brine injection (iv). (c) Segmented images delineating the oil (green), brine (blue), and grains (black) corresponding to each stage in (b) are obtained through image processing. Due to the two-dimensional nature of the micromodel platform, segmented images delineating the area of each phase enables quantification for volumetric saturations of the crude oil, S_o, and brine, S_w. (d) Oil recoveries calculated from the segmented images across the micromodel show an initial oil recovery of ~38% OOIP, followed by an increase of ~6.5% OOIP after the low salinity waterflood, and an increase of ~8% OOIP after the freshwater injection due to flow diversion from the spontaneous Pickering emulsification of the crude oil.

macroscopic water films. Of particular interest to the industry, we discover that the mobilized clay particles at low salinity (freshwater) conditions act to stabilize the oil-water interface and enable spontaneous generation of Pickering emulsions in the preferential flow paths. The Pickering emulsions are characterized and stable over long times. Spontaneous emulsification in preferential flow paths reduces the local apparent permeability and thus requires a large pressure differential for flow. As a result, flow is diverted to oil-filled pores that become amenable for flow at smaller pressure gradient. The overall effect of the spontaneous Pickering emulsification and flow diversion is quantified, showing an additional increase in oil recovery of ~8% OOIP.

Acknowledgements

This work is supported by the SURPI-A Industrial Affiliates. W. Song gratefully acknowledges the financial support of the Gerald J. Lieberman Fellowship and the Hormoz and Fariba Ameri Graduate Fellowship.

References

[1] E. Hilner, M.P. Andersson, T. Hassenkam, J. Matthiesen, P.A. Salino, S.L.S. Stipp, The effect of ionic strength on oil adhesion in sandstone - the search for the low salinity mechanism, Scientific Reports 5 (9933).
[2] G.-Q. Tang, N.R. Morrow, Influence of brine composition and fines migration on crude oil/brine/rock interactions and oil recovery, J. Petrol. Sci. Eng. 24 (1999) 99–111.
[3] T. Amirian, M. Haghighi, P. Mostaghimi, Pore scale visualization of low salinity water flooding as an enhanced oil recovery method, Energy Fuels 31 (12) (2017) 13133–13143, https://doi.org/10.1021/acs.energyfuels.7b01702.
[4] W.-B. Bartels, H. Mahani, S. Berg, R. Menezes, J.A. van der Hoeven, A. Fadili, Oil configuration under high-salinity and low-salinity conditions at pore scale: a parametric investigation by use of a single-channel micromodel, SPE J. 22 (05) (2017) 1362–1373, https://doi.org/10.2118/181386-PA.
[5] S. Boussour, M. Cissokho, C. Philippe, H.J. Bertin, G. Hamon, Oil recovery by low salinity brine injection: Laboratory results outcrop and reservoir cores, SPE Annual Technical Conference and Exhibition, 4-7 October, New Orleans, Louisiana doi:10.2118/124277-MS.
[6] A. Fogden, M. Kumar, N.R. Morrow, J.S. Buckley, Mobilization of fine particles during flooding of sandstones and possible relations to enhanced oil recovery, Energy Fuels 25 (4) (2011) 1605–1616 doi:10.1021/ef101572n.
[7] S.B. Fredriksen, A.U. Rognmo, M.A. Fernø, Pore-scale mechanisms during low salinity waterflooding: Oil mobilization by diffusion and osmosis, J. Petrol. Sci. Eng. 163 (2018) 650–660.
[8] A. Lager, K. Webb, C. Black, Impact of Brine Chemistry on Oil Recovery, in: IOR 2007-14th European Symposium on Improved Oil Recovery (2007).
[9] A. Lager, K.J. Webb, R.I. Collins, D.M. Richmond, LoSal enhanced oil recovery: evidence of enhanced oil recovery at the reservoir scale, SPE Symposium on Improved Oil Recovery, 20-23 April, Tulsa, Oklahoma, USAdoi:10.2118/113976-MS.
[10] A. Emadi, M. Sohrabi, Visual investigation of oil recovery by lowsalinity water injection: formation of water micro-dispersions and wettability alteration, in: SPE Annual Technical Conference and Exhibition, no. 1999, New Orleans, LA, 2013, pp. 1–15.
[11] D. Sinton, Energy: the microfluidic frontier, Lab Chip 14 (17) (2014) 3127–3134 doi:10.1039/c4lc00267a.
[12] B. Vega, A. Dutta, A.R. Kovscek, CT imaging of low-permeability, dual-porosity systems using high X-ray contrast gas, Transport Porous Media 101 (1) (2014) 81–97, https://doi.org/10.1007/s11242-013-0232-0.
[13] P. Nguyen, H. Fadaei, D. Sinton, Microfluidics underground: a micro-core method for pore scale analysis of supercritical CO2 reactive transport in saline aquifers, J. Fluids Eng. 135 (2) (2013) 021203, https://doi.org/10.1115/1.4023644.
[14] X. Chen, S. Gao, A. Kianinejad, D.A. DiCarlo, Steady-state supercritical CO2 and brine relative permeability in Berea sandstone at different temperature and pressure conditions, Water Resour. Res. 53 (7) (2003) 6312–6321.
[15] D. DiCarlo, S. Akshay, M. Blunt, Three-Phase Relative Permeability of Water-Wet, Oil-Wet, and Mixed-Wet Sandpacks, Society of Petroleum Engineers 5 (01). doi:10.2118/60767-PA.
[16] M. Buchgraber, M. Al-Dossary, C. Ross, A.R. Kovscek, Creation of a dual-porosity micromodel for pore-level visualization of multiphase flow, J. Petrol. Sci. Eng. 86-87 (2012) 27–38.
[17] W. Song, T.W. de Haas, H. Fadaei, D. Sinton, Chip-off-the-old-rock: the study of reservoir-relevant geological processes with real-rock micromodels, Lab Chip 14 (22) (2014) 4382–4390, https://doi.org/10.1039/C4LC00608A.
[18] M.L. Porter, J. Jiménez-Martínez, R. Martinez, Q. McCulloch, J.W. Carey, H.S. Viswanathan, Geo-material microfluidics at reservoir conditions for subsurface energy resource applications, Lab Chip 15 (20) (2015) 4044–4053.
[19] S.A. Mahoney, T.E. Rufford, V. Rudolph, K.Y. Liu, S. Rodrigues, K.M. Steel, Creation of microchannels in Bowen Basin coals using UV laser and reactive ion etching, Int. J. Coal Geol. 144-145 (2015) 48–57.
[20] W. Song, A.R. Kovscek, Functionalization of micromodels with kaolinite for investigation of low salinity oil-recovery processes, Lab Chip 15 (2015) 3314–3325, https://doi.org/10.1039/C5LC00544B.
[21] W. Song, A.R. Kovscek, Direct visualization of pore-scale fines migration and formation damage during low-salinity waterflooding, J. Nat. Gas Sci. Eng. 34 (2016) 1276–1283, https://doi.org/10.1016/j.jngse.2016.07.055.
[22] S.G. Lee, H. Lee, A. Gupta, S. Chang, P.S. Doyle, Site-Selective In Situ Grown Calcium Carbonate Micromodels with Tunable Geometry, Porosity, and Wettability, Advanced Functional Materialsdoi:10.1002/adfm.201600573. URL http://doi.wiley.com/10.1002/adfm.201600573.
[23] W. Song, F. Ogunbanwo, M. Steinsbø, M.A. Fernø, A.R. Kovscek, Mechanisms of multiphase reactive flow using biogenically calcite-functionalized micromodels, Lab Chip doi:10.1039/c8lc00793d.
[24] M. Buchgraber, Microvisual investigations to assess and understand enhanced oil recovery processes using etched silicon micromodels, Ph.D. thesis, Stanford University, 2013.
[25] J. Peng, Heavy-Oil Solution Gas Drive and Fracture Reconsolidation of Diatomite During Thermal Operations, Ph.D. thesis, Stanford University, 2009.
[26] X.-m. Zhou, O. Torsaeter, X. Xie, N. Morrow, The Effect of Crude-Oil Aging Time and Temperature on the Rate of Water Imbibition and Long-Term Recovery by Imbibition, SPE Formation Evaluation 10 (04). doi:doi.org/10.2118/26674-PA.
[27] X. Zhou, N. Morrow, S. Ma, Interrelationship of wettability, initial water saturation,

aging time, and oil recovery by spontaneous imbibition and waterflooding, SPE J. 5 (2) (2000) 21–24, https://doi.org/10.2118/62507-PA.
[28] A.R. Kovscek, H. Wong, C.J. Radke, A pore-level scenario for the development of mixed wettability in oil reservoirs, AIChE J. 39 (6) (1993) 1072–1085 doi:10.1002/aic.690390616.
[29] S. Pickering, Emulsions, J. Chem. Soc. Trans. 91 (1907) 2001–2021.
[30] Y. Chevalier, M.-A. Bolzinger, Emulsions stabilized with solid nanoparticles: Pickering emulsions, Colloids Surf. A: Physicochem. Eng. Aspects 439 (2013) 23–34.
[31] R.H. Worden, S. Morad, Clay mineral cements in sandstones, Int. Assoc. Sedimentologists (2009).
[32] A. Lager, K.J. Webb, C.J.J. Black, M. Singleton, K.S. Sorbie, Low salinity oil recovery - an experimental investigation, Petrophysics 49 (1) (2008) 28–35.
[33] N.J. Hadia, T. Hansen, M.T. Tweheyo, Influence of crude oil components on recovery by high and low salinity water flooding, Energy Fuels 26 (2012) 4328–4335.